J|A|C|S ARTICLES

Published on Web 09/09/2009

Enhanced In situ Continuous-Flow MAS NMR for Reaction Kinetics in the Nanocages

Shutao Xu,[†,‡] Weiping Zhang,[*,†] Xianchun Liu,[†] Xiuwen Han,[†] and Xinhe Bao[*,†]

State Key Laboratory of Catalysis, Dalian Institute of Chemical Physics, Chinese Academy of Sciences, 457 Zhongshan Road, Dalian 116023, China, and Graduate University of Chinese Academy of Sciences, Beijing 100049, China

Received May 27, 2009; E-mail: wpzhang@dicp.ac.cn; xhbao@dicp.ac.cn

Abstract: A new approach of in situ continuous-flow laser-hyperpolarized ^{129}Xe MAS NMR together with ^{13}C MAS NMR is designed and applied successfully to study the adsorption and reaction kinetics in the nanospace. Methanol conversion in CHA nanocages has been investigated in detail for proof of principle demonstrating the prospect of in situ NMR of reaction kinetics. Our findings well elucidates that the reaction intermediate can be identified by ^{13}C MAS NMR spectroscopy, meanwhile the kinetic and dynamic processes of methanol adsorption and reaction in CHA nanocages can be monitored by one- and two-dimensional hyperpolarized ^{129}Xe MAS NMR spectroscopy under the continuous-flow condition close to the real heterogeneous catalysis. The kinetic curves and apparent activation energy of the nanocages involving the active site are obtained quantitatively. The advantages of hyperpolarized ^{129}Xe with much higher sensitivity and shorter acquisition time allow the kinetics to be probed in a confined geometry under real working conditions.

1. Introduction

The nanostructures under confinement are the subject of continuing interest because they are remarkably different from those in the corresponding bulk space and have various potential applications in optical and electrical devices, catalytic reactions, etc.[1−4] Noninvasive measurements of reaction kinetics in a confined space by in situ spectroscopy are therefore of great significance. In situ magic-angle spinning (MAS) NMR spectroscopy is a powerful tool for investigating the catalytic reactions at high temperatures; progress has been made in the development and application of the in situ NMR approach under batchlike or continuous-flow mode.[5−11] Most of these studies are focused on the reactant transformation and/or intermediate detection while less information of the catalytic kinetics is reported under the condition of continuous-flow close to the real heterogeneous catalytic process. Reaction kinetics from the conventional ^{1}H and ^{13}C NMR is obtained by the concentration variations of reactant or product in the bulk state,[12] however, the kinetics in a confined space such as nanocage or nanochannel can not be achieved easily. It has been shown that laser-hyperpolarized (HP) ^{129}Xe NMR technique is powerful in studying the porosity of porous materials,[13−17] or even diffusion and combustion process.[18,19] The resultant ^{129}Xe NMR spectrum is from xenon atoms adsorbed in the pores with dimensions down to the nanoscale, which could make it possible for investigation of the reaction kinetics in a restricted geometry. In this study, we report a design of laser-hyperpolarized ^{129}Xe mixed with a reactant under continuous flow to investigate the catalytic kinetics including adsorption and reaction processes in nanocages by in situ magic-angle spinning (MAS) NMR. In our strategy, laser-hyperpolarized xenon is achieved by spin-exchange optical pumping to tremendously enhance the signal intensity by 4−5 orders of magnitude compared to conventional

[†] Dalian Institute of Chemical Physics.
[‡] Graduate University of Chinese Academy of Sciences.

(1) Hu, J.; Odom, T. W.; Lieber, C. M. *Acc. Chem. Res.* **1999**, *32*, 435–445.
(2) Bell, A. T. *Science* **2003**, *299*, 1688–1691.
(3) Schlögl, R.; Hamid, S. B. A. *Angew. Chem., Int. Ed.* **2004**, *43*, 1628–1637.
(4) Pan, X. L.; Bao, X. H. *Chem. Commun.* **2008**, 6271–6281.
(5) Hunger, M.; Horvath, T. *J. Chem. Soc., Chem. Commun.* **1995**, 1423–1424.
(6) Haw, J. F.; Goguen, P. W.; Xu, T.; Skloss, T. W.; Song, W.; Wang, Z. *Angew. Chem., Int. Ed.* **1998**, *37*, 948–949.
(7) Zhang, W. P.; Ma, D.; Liu, X. C.; Liu, X. M.; Bao, X. H. *Chem. Commun.* **1999**, 1091–1092.
(8) Ma, D.; Shu, Y. Y.; Zhang, W. P.; Han, X. W.; Xu, Y. D.; Bao, X. H. *Angew. Chem., Int. Ed.* **2000**, *39*, 2928–2931.
(9) Haw, J. F.; Song, W.; Marcus, D. M.; Nicholas, J. B. *Acc. Chem. Res.* **2003**, *36*, 317–326.
(10) Xu, M. C.; Harris, K. D. M.; Thomas, J. M.; Vaughan, D. E. W. *ChemPhysChem* **2007**, *8*, 1311–1313.
(11) Wang, W.; Hunger, M. *Acc. Chem. Res.* **2008**, *41*, 895–904.
(12) Luzgin, M. V.; Stepanov, A. G.; Arzumanov, S. S.; Rogov, V. A.; Parmon, V. N.; Wang, W.; Hunger, M.; Freude, D. *Chem.—Eur. J.* **2006**, *12*, 457–465.
(13) Moudrakovski, I. L.; Terskikh, V. V.; Ratcliffe, C. I.; Ripmeester, J. A.; Wang, L. Q.; Shin, Y.; Exarhos, G. J. *J. Phys. Chem. B* **2002**, *106*, 5938–5946.
(14) Nossov, A.; Guenneau, F.; Springuel-Huet, M. A.; Haddad, E.; Montouillout, V.; Knott, B.; Engelke, F.; Fernandez, C.; Gedeon, A. *Phys. Chem. Chem. Phys.* **2003**, *5*, 4479–4483.
(15) Zhang, W. P.; Ratcliffe, C. I.; Moudrakovski, I. L.; Mou, C. Y.; Ripmeester, J. A. *Anal. Chem.* **2005**, *77*, 3379–3382.
(16) Liu, Y.; Zhang, W. P.; Xie, S. J.; Xu, L. Y.; Han, X. W.; Bao, X. H. *J. Phys. Chem. B.* **2008**, *112*, 1226–1231.
(17) Liu, Y.; Zhang, W. P.; Liu, Z. C.; Xu, X. T.; Wang, Y. D.; Xie, Z. K.; Han, X. W.; Bao, X. H. *J. Phys. Chem. C.* **2008**, *112*, 15375–15381.
(18) Meersmann, T.; Logan, J. W.; Simonutti, R.; Caldarelli, S.; Comotti, A.; Sozzani, P.; Kaiser, L. G.; Pines, A. *J. Phys. Chem. A* **2000**, *104*, 11665–11670.
(19) Anala, S.; Pavlovskaya, G. E.; Pichumani, P.; Dieken, T. J.; Olsen, M. D.; Meersmann, T. *J. Am. Chem. Soc.* **2003**, *125*, 13298–13302.

 10.1021/ja904304h CCC: $40.75

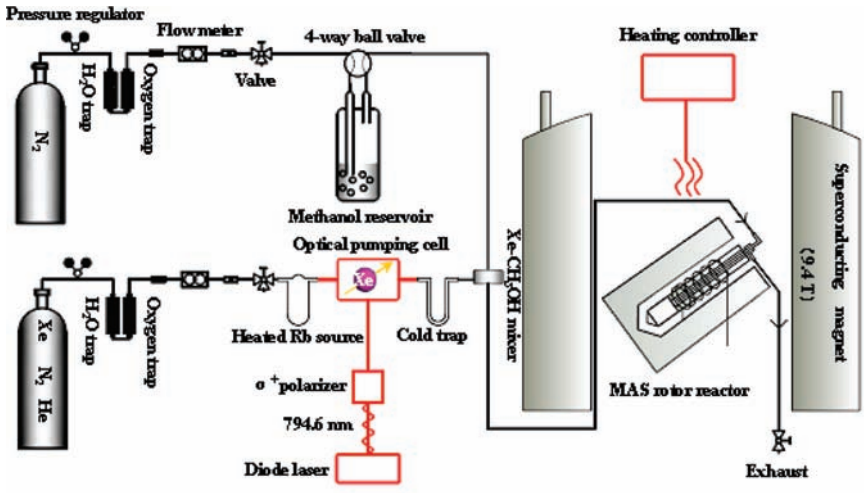

Figure 1. Sketch of the experimental setup for in situ continuous-flow MAS NMR study.

^{129}Xe NMR.[20−22] Then HP ^{129}Xe is premixed with a reactant outside the probe head and enters the high-field coil region with an MAS NMR rotor where the catalyst is located (Figure 1). In this case, it is possible for us to monitor the catalytic process in a confined space at the earliest stage by HP ^{129}Xe NMR spectroscopy with much higher sensitivity and shorter acquisition time (∼10 s per spectrum). Here, methanol conversion in CHA-structured nanocages is used for proof of principle demonstrating the prospect of in situ NMR of reaction kinetics. This provides a feasible approach to investigate the reaction kinetics in a confined geometry under real working conditions.

2. Experimental Section

2.1. In situ Continuous-Flow MAS NMR Experiment. H-type CHA zeolite (Si/Al: 15.0) with the cage dimension of 7.5 × 8.2 Å and 8-membered-ring window dimension of 4.4 × 3.6 Å (see the Supporting Information, Scheme SI-1) was provided by BASF company (Germany). Prior to the in situ MAS NMR experiments, about 100 mg samples were dehydrated at 400 °C for 20 h in a vacuum (<1 × 10^{-2} Pa). As we previously reported in refs 15−17, laser-hyperpolarized ^{129}Xe was achieved with the optical pumping cell in the fringe field of spectrometer magnet and 60 W diode laser array (Coherent). A continuous flow of a 1% Xe−1% N_2−98% He gas mixture was delivered at the rate of 100 mL/min to the rotor reactor with or without 99% enriched $^{13}CH_3OH$ (Cambridge Isotopes) bubbled with dry nitrogen at the rate of 10 mL/min (Figure 1).

2.2. In situ MAS NMR Measurements. All NMR spectra were collected on Varian Infinityplus-400 spectrometer. The in situ probe was modified according to that reported by Hunger et al.[5] One-dimensional HP^{129}Xe MAS NMR spectra were accumulated at 110.6 MHz with a $\pi/2$ pulse width of 3 μs, a 1 s recycle delay and 10 scans. The samples were spun at 3 kHz under continuous flow using a 7.5 mm rotor. The chemical shifts were referenced to the signal of xenon gas. Although this line was temperature-dependent, its chemical shift variation would not be more than 1 ppm in the whole range of measurements because of the very low concentration of xenon. The two-dimensional exchange experiments (2D-EXSY) were performed using a $90°-t_1-90°-\tau_m-90°-t_2$ pulse sequence in TPPI mode. ^{13}C CP/MAS NMR spectra were recorded with a $\pi/4$ pulse width of 1.5 μs, a contact time of 1 ms, a recycle delay of 2 s, and 16−64 scans. The chemical shifts of ^{13}C NMR spectra were referenced to adamantane with the upfield methine peak at 29.5 ppm.

3. Results and Discussion

3.1. Kinetics of Methanol Adsorption in CHA Nanocages. Figure 2 shows the in situ HP ^{129}Xe MAS NMR spectra recording the evolution of diffusion and adsorption of methanol in CHA nanocages at room temperature. The peaks at 0 ppm in the ^{129}Xe NMR spectra are from xenon in the gas phase. All signals at lower field are originated from the adsorbed xenon in the CHA nanocages. Before introduction of ^{13}C-enriched methanol, the chemical shift of ^{129}Xe in empty cages is 84 ppm. Its chemical shift is nearly unchanged with increasing temperatures (see the Supporting Information, Figure SI-1). This can be attributed to the restriction of the 8-membered-ring window of the cage not allowing more Xe atoms to diffuse inside, and thus the interaction between Xe atoms can be neglected. After methanol is coinjected with the HP xenon into the rotor reactor, another signal appears at the lower field that can be attributed to Xe coadsorbed with methanol in the CHA cages. With increasing the adsorption time, its intensity increases, whereas that of xenon in empty cages decreases. Finally, after about 15 min, there is only one peak whose chemical shift is ca. 99 ppm, which indicates that the adsorption of methanol reaches steady state. The adsorption of methanol in CHA nanocages can be described as follows

$$CH_3OH(g) + [Cage]_{empty} \rightarrow CH_3OH@[Cage] \qquad (1)$$

where CH_3OH (g) stands for methanol in the gas phase, $[Cage]_{empty}$ denotes the CHA cages without adsorption of methanol.

For quantitatively obtaining the kinetic information of methanol adsorption in the CHA cages, continuous-flow HP ^{129}Xe MAS NMR spectra were also recorded at 60 and 100 °C, respectively (see the Supporting Information, Figures SI-2 and SI-3). The spectra have similar features when increasing the temperature, but the time of methanol adsorption to steady state is shortened a little. Appropriate integration of the ^{129}Xe NMR spectra yields the concentration of Xe in empty cages without methanol as a function of time. The kinetic curves of methanol adsorbed in CHA nanocages can be fitted with second order

(20) Happer, W.; Miron, E.; Schaefer, S.; Schreiber, D.; van Wingaarden, W. A.; Zeng, X. *Phys. Rev. A* **1984**, *29*, 3092–3110.
(21) Raftery, D.; Long, H.; Meersmann, T.; Grandinetti, P. J.; Reven, L.; Pines, A. *Phys. Rev. Lett.* **1991**, *66*, 584–587.
(22) Raftery, D.; MacNamara, E.; Fisher, G.; Rice, C. V.; Smith, J. *J. Am. Chem. Soc.* **1997**, *119*, 8746–8747.

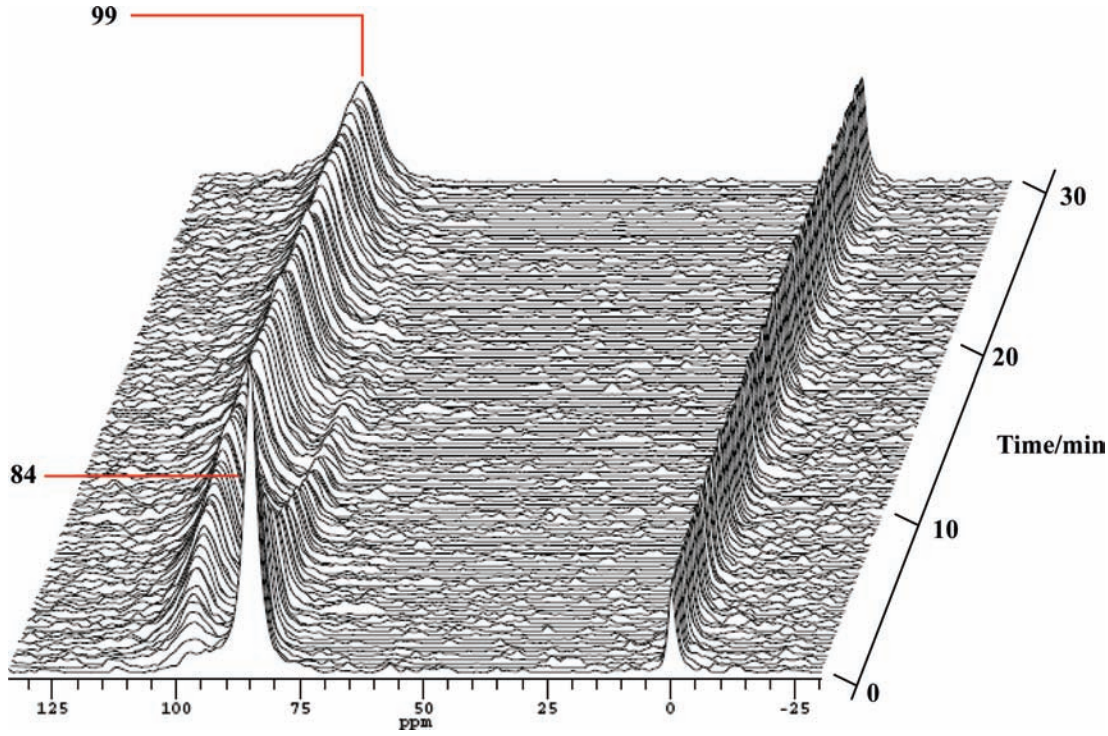

Figure 2. In situ HP ^{129}Xe MAS NMR spectra recorded with time resolution of 10 s per spectrum as a function of time during adsorption of methanol in CHA nanocages at 25 °C.

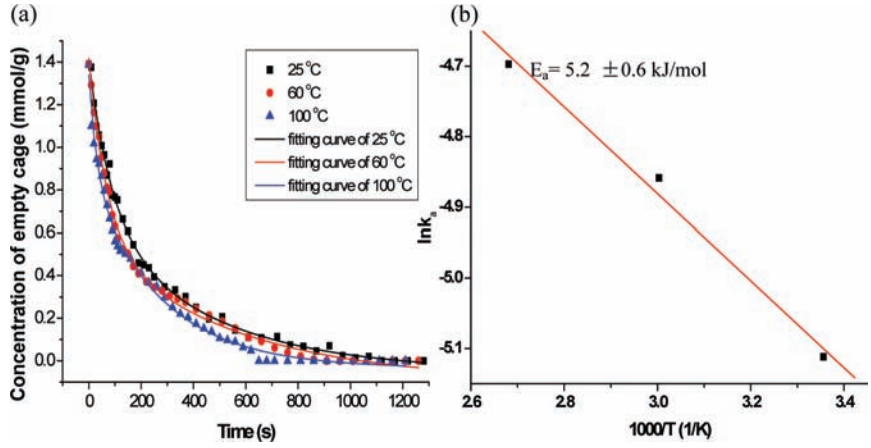

Figure 3. (a) Kinetic curves of methanol adsorption in the CHA nanocages at various temperatures. (b) Arrhenius plot of rate constant k_a at different adsorption temperatures, E_a is the adsorption activation energy.

exponential decay function (Figure 3a). Furthermore, the rate function of methanol adsorbed in the CHA nanocages can be expressed by $r = k_1[CH_3OH]_g{}^m[Cage]^n{}_{empty}$, where k_1 is adsorption rate constant, $[CH_3OH]_g$ is the concentration of methanol in the gas phase, and $[Cage]_{empty}$ is the concentration of empty cage without methanol. $[CH_3OH]_g$ remains constant due to the continuous injection of methanol vapor into the rotor by N_2, thus $r = k_a[Cage]^n{}_{empty}$, where $k_a = k_1\ [CH_3OH]_g{}^m$. Thus, the adsorption rate function at different temperatures can be obtained as $r = k_a[Cage]^{1.57}{}_{empty}$ after fitting the kinetic curves in Figure 3a. The adsorption constants (k_a) are listed in Figure 3b. The activation energy of methanol adsorption in the CHA nanocages could be estimated as *ca.* 5.2 kJ/mol according to the Arrhenius equation (Figure 3b). It is in the physical adsorption range.

3.2. Kinetics of Methanol Reaction in CHA Nanocages. After saturation adsorption of methanol, the temperature is gradually increased from 25 to 200 °C by the instrument heating system while the gas mixture of $^{13}CH_3OH$ and HP ^{129}Xe is injected. ^{13}C CP/MAS NMR spectra (Figure 4) show that below 120 °C, only methanol with chemical shift at 50.5 ppm can be observed; above 120 °C, methanol can be converted into dimethyl ether (DME) whose chemical shift is at 60.5 ppm via the methoxy whose chemical shift is at 56.8 ppm and that plays a role as the intermediate.[23] More and more methanol is transformed to DME with increasing temperatures. Interestingly, in the HP ^{129}Xe NMR spectra the signal splits into two peaks when DME is produced at 120 °C: one main peak named A is at lower field, the other shoulder peak named B is at higher field. Peak A is from Xe coadsorbed with methanol in CHA cages. It shifts a little to higher field with increasing temperature because of the desorption of methanol and more free voids left. The relative

(23) Wang, W.; Seiler, M.; Hunger, M. *J. Phys. Chem. B.* **2001**, *105*, 12553–12558.

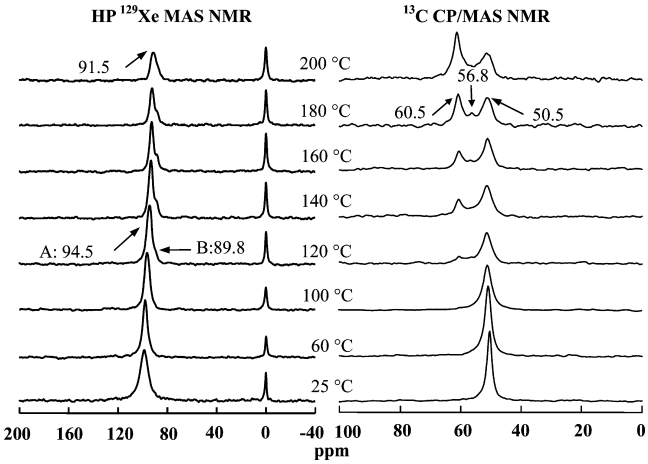

Figure 4. In situ HP ^{129}Xe MAS NMR and ^{13}C CP/MAS NMR spectra of methanol reaction in CHA nanocages at various temperatures.

intensity of peak B is increased with increasing temperatures. From the combination of ^{129}Xe and ^{13}C CP/MAS NMR spectra, peak B in the ^{129}Xe NMR spectra may be due to the occurrence of the methanol conversion. With increasing temperatures, ^{13}C CP/MAS NMR spectra show that methanol tends to be desorbed, and more DME is produced. Thus, at 200 °C in the HP ^{129}Xe NMR spectra the chemical shift of the methanol adsorption signal further decreases, and these two peaks can not be well resolved.

To further confirm the assignment of peak B, we acquired in situ two-dimensional HP ^{129}Xe exchange spectra (2D-EXSY)[24] during methanol conversion under the steady state. The technique can be extended to investigate the dynamic processes of xenon in different domains in the porous materials.[16,17,19,25] The cross-peaks indicate an exchange of xenon atoms between the corresponding environments on the diagonal within the period of mixing time. At the reaction temperature of 180 °C, the presence of cross-peaks in Figure 5a suggests that the exchange of Xe between gas phase and peak A exists at a time scale of 30 ms. Another cross-peak emerging in Figure 5c indicates that the exchange of Xe between gas phase and peak B occurs when increasing mixing time to 80 ms. Therefore, xenon exchange takes place faster between gas phase and peak A than between gas phase and peak B. This could be caused by the desorption of products, which restricts the xenon atoms motion between the gas phase and the CHA cages. So, it further confirms that the new peak B can be assigned to xenon in the methanol reaction cage, in which methanol molecules are converted to DME and water on the Brönsted acid site.

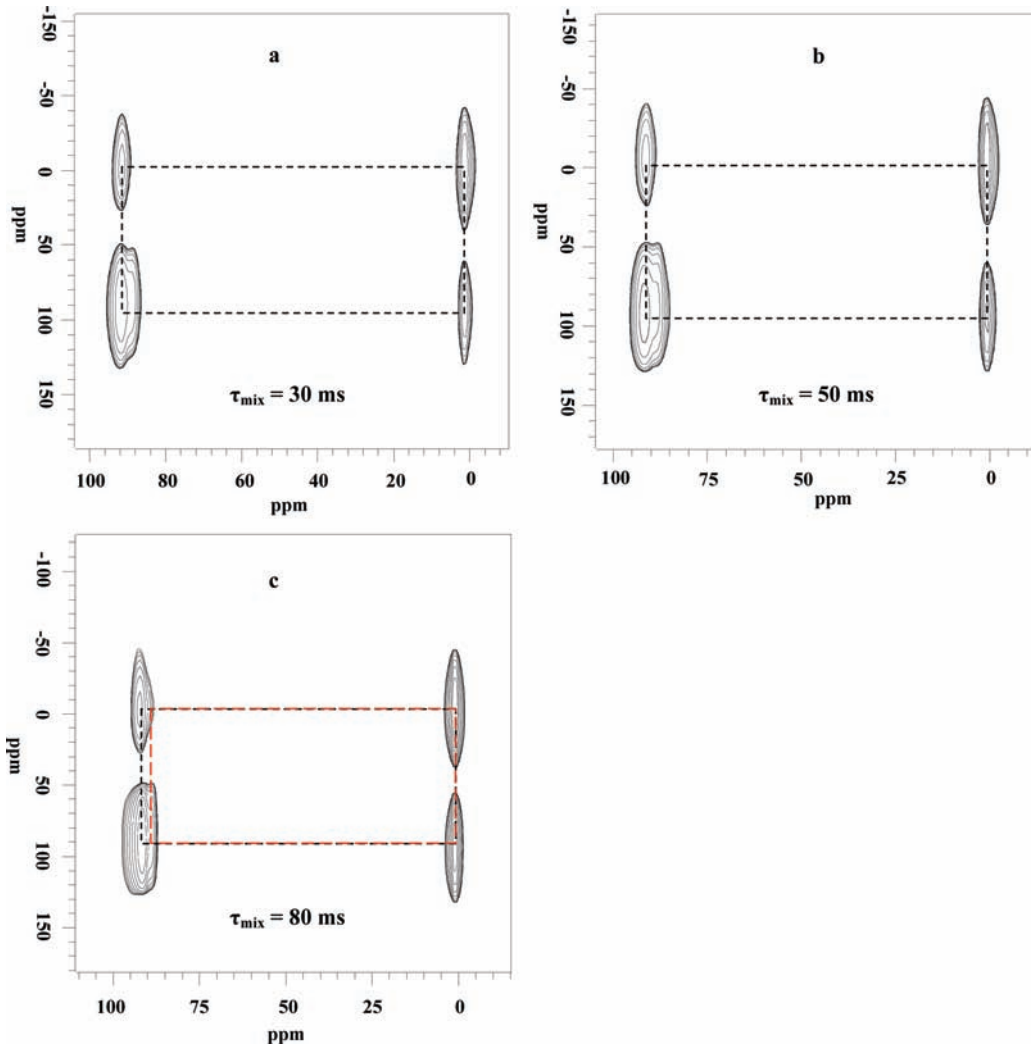

Figure 5. In situ HP ^{129}Xe 2D-EXSY MAS NMR spectra recorded during methanol reaction in CHA nanocages at 180 °C with different mixing time. The black dashed lines denote Xe exchange between gas phase and peak A, and the red ones denote Xe exchange between gas phase and peak B.

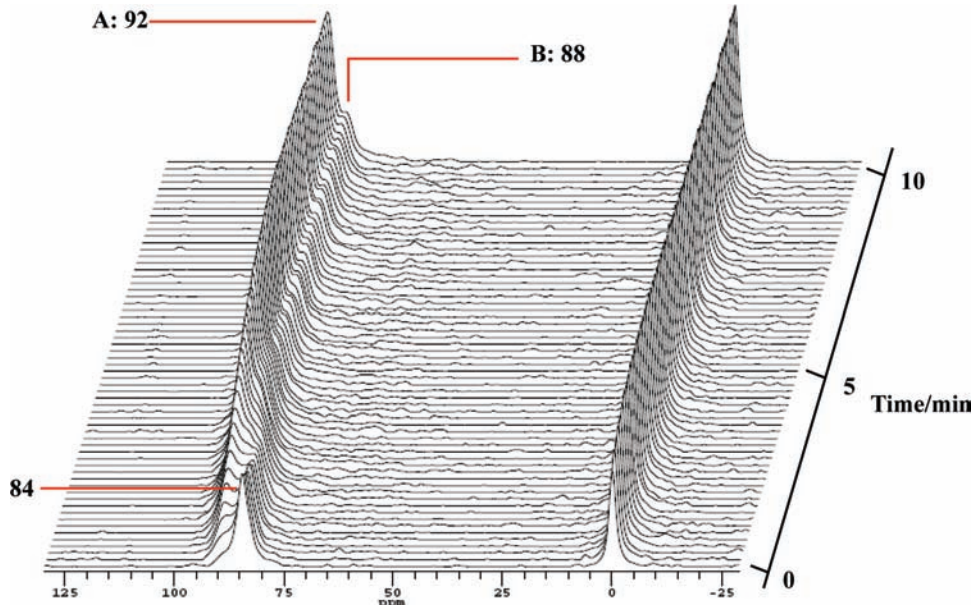

Figure 6. In situ HP ^{129}Xe MAS NMR spectra recorded with time resolution of 10 s per spectrum as a function of time during reaction of methanol in CHA nanocages at 180 °C.

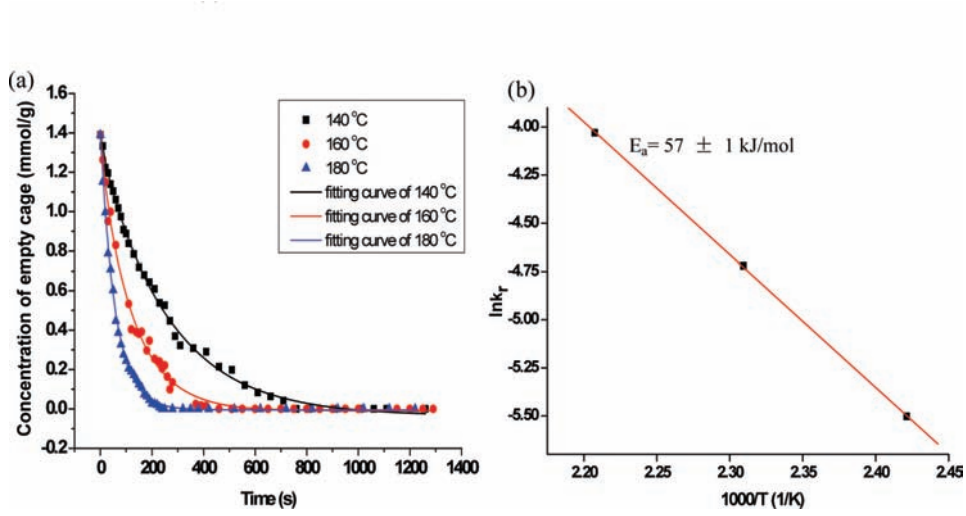

Figure 7. (a) Kinetic curves of methanol reaction in CHA nanocages at various temperatures. (b) Arrhenius plot of rate constants k_r at different reaction temperatures, E_a is the apparent reaction activation energy.

To trace the reaction kinetics, in situ HP ^{129}Xe MAS NMR spectra were recorded as a function of time to map the evolution of methanol conversion in the CHA nanocages at 180 °C (Figure 6). The empty cage signal at 84 ppm decreases in intensity with the time, while the signals of methanol adsorbed cage at 92 ppm and methanol reaction cage at 88 ppm increase. When the intensity of empty cage decreases to zero, the intensities of the other two signals are unchanged with increasing time. Similar phenomena can be observed at 140 and 160 °C (see the Supporting Information, Figures SI-4 and SI-5). According to the theoretical and experimental studies on this reaction,[23,26,27] one of the reasonable energetic routes for methanol conversion to DME is the indirect pathway, i.e., methanol adsorbed on an acid site reacts first to methoxy species, which subsequently converts with another methanol molecule to DME. In our case, methanol conversion is in a nonequilibrium steady state because methanol is continuously injected into the nanocages, methanol continuously reacts to DME and water via methoxy, and products continuously leave the nanocages. So, the methanol reaction in CHA nanocages can be proposed as follows

$$CH_3OH(g) + [Cage]_{empty} \rightarrow CH_3OH@[Cage] \quad (1)$$

$$CH_3OH@[Cage] \rightarrow CH_3O\&H_2O@[Cage] \quad (2)$$

$$CH_3OH(g) + CH_3O\&H_2O@[Cage] \rightarrow DME\&H_2O@[Cage] \quad (3)$$

$$2CH_3OH(g) + [Cage]_{empty} \rightarrow DME\&H_2O@[Cage] \quad (4)$$

$$DME\&H_2O@[Cage] \rightarrow DME\&H_2O + [Cage]_{empty} \quad (5)$$

Equation 4 is the overall reaction of elementary steps 1−3 for methanol conversion in CHA nanocages, including the adsorption and reaction of methanol; the following step is the desorption of DME and water to recover the empty cage. The desorption of products should take place rapidly, which is not

a rate-determining step because the conversion of methanol reaches the steady state as shown by the presence of a signal at 88 ppm in Figure 6, and there is no coke observed in the ^{13}C CP/MAS NMR spectra (Figure 4). So, only eq 4 has been considered for the kinetic analysis. The reaction rate function can be expressed as $r = k_2[CH_3OH]_g^m[Cage]^n_{empty}$, where k_2 denotes the apparent reaction rate constant. Similarly, $[CH_3OH]_g$ can be regarded as a constant, thus $r = k_r[Cage]^n_{empty}$, where $k_r = k_2[CH_3OH]_g^m$. Clearly, the reaction rate of methanol conversion depends on the concentration of the empty cages in CHA zeolite. In our case, CHA zeolite with a Si/Al ratio of 15 has nearly one Brönsted acid site in each cage. Moreover, both the adsorption and reaction processes are involved in the Brönsted acid site, which plays a role as the active site. Therefore, the concentration of empty cage can represent the amount of active site. The above reaction rate function indicates that the methanol conversion rate is dependent on the concentration of active site. Prior to kinetic analysis, the effect of internal and external diffusion could be excluded because of the fine catalyst particles and fast gas flow (ca. 110 mL/min). In the same way, the kinetic curves of the reaction process are exhibited in Figure 7a. Thus, the reaction rate function with different temperatures can also be obtained as $r = k_r[Cage]^{1.27}_{empty}$ after fitting the kinetic curves in Figure 7a. Therefore, the apparent activation energy of active site in methanol reaction could be calculated as ca. 57 kJ/mol according to the Arrhenius equation (Figure 7b). This value is a little lower compared to other studies which show the methanol conversion on Al_2O_3 or H-type zeolite with the activation energy of the overall reaction from 58 to 143 kJ/mol.[28−30] In our study, the empty CHA nanocage represents the active site and is described in the reaction rate function from the molecular level that is different from the other conventional kinetic studies, which concern only the concentration of reactants or products in the bulk space. Our approach demonstrates the reaction kinetics in the nanocages with continuous flow of reactants. The advantages of HP ^{129}Xe with much higher sensitivity and shorter acquisition time allow the kinetics of the active site in a confined space to be probed at the earliest reaction stage.

4. Conclusions

In summary, a design of in situ continuous-flow laser-hyperpolarized ^{129}Xe MAS NMR coupled with ^{13}C MAS NMR is successfully applied to study the adsorption and reaction kinetics in a confined space. Our approach well elucidates that the reaction intermediate can be identified by ^{13}C MAS NMR, in the mean time, the kinetic and dynamic processes of methanol adsorption and conversion in the CHA nanocages can be monitored by one- and two-dimensional hyperpolarized ^{129}Xe MAS NMR under the continuous-flow condition close to the real heterogeneous catalysis. The kinetic curves and apparent activation energy of the nanocage with the active site are obtained because of the advantages of hyperpolarized xenon having much higher sensitivity and subsequently shorter acquisition time. We believe this approach can be extended to the other reactions and generally applied in the investigation of reaction kinetics in a restricted geometry under real working conditions.

Acknowledgment. We thank Prof. Shang-Bin Liu (Academia Sinica, Taiwan) for helpful discussions with the hyperpolarized ^{129}Xe optical pumping system. We also thank Dr. Ulrich Mueller of BASF company, Germany for kindly providing the zeolite samples. We are grateful for the financial support of the National Natural Science Foundation of China (20573106, 20873140) and Ministry of Science and Technology of China through the National Key Project of Fundamental Research (2003CB615806, 2009CB623507).

Supporting Information Available: Topological scheme of CHA zeolite, HP ^{129}Xe MAS NMR spectra of CHA zeolite before introduction of methanol at various temperatures, HP ^{129}Xe MAS NMR spectra of methanol adsorption in CHA nanocages at 60 and 100 °C, HP ^{129}Xe MAS NMR spectra of methanol reaction in CHA nanocages at 140 and 160 °C. This material is available free of charge via the Internet at http://pubs.acs.org.

JA904304H

(24) Jeener, J.; Meier, B. H.; Bachmann, P.; Ernst, P. R. *J. Chem. Phys.* **1979**, *71*, 4546–4553.
(25) Knagge, K.; Smith, J. R.; Smith, L. J.; Buriak, J.; Raftery, D. *Solid State Nucl. Magn. Reson.* **2006**, *29*, 85–89.
(26) Ivanova, I. I.; Corma, A. *J. Phys. Chem.* **1997**, *101*, 547–551.
(27) Boronat, M.; Martínez-Sánchez, C.; Law, D.; Corma, A. *J. Am. Chem. Soc.* **2008**, *130*, 16316–16323.
(28) Bercic, G.; Levec, J. *Ind. Eng. Chem. Res.* **1992**, *31*, 1035–1040.
(29) Lee, E. Y.; Park, Y. K.; Joo, O. S.; Jung, K. D. *React. Kinet. Catal. Lett.* **2006**, *89*, 115–121.
(30) Xu, M. T.; Lunsford, J. H.; Goodman, D. W.; Bhattacharyya, A. *Appl. Catal., A* **1997**, *149*, 289–301.